CHIN. PHYS. LETT. Vol. 30, No. 6 (2013) 060302

Continuous Variable Entanglement Distribution for Long-Distance Quantum Communication *

ZHAO Jun-Jun(赵军军), GUO Xiao-Min(郭晓敏), WANG Xu-Yang(王旭阳), WANG Ning(王宁), LI Yong-Min(李永民)**, PENG Kun-Chi(彭堃墀)

State Key Laboratory of Quantum Optics and Quantum Optics Devices, Institute of Opto-Electronics, Shanxi University, Taiyuan 030006

(Received 5 February 2013)

We develop a frequency-tunable two-color continuous variable entangled state and demonstrate the entanglement distribution over a telecom single mode fiber. One beam of the entangled state (795 nm) can be continuously tuned over a range of 2.4 GHz and the hyperfine transitions of a rubidium D1 line are measured based on saturated absorption spectroscopy. The other beam (1560 nm) is injected into a 5-km single mode fiber to distribute the entanglement, and the entanglement evolution between the transmitted beam and its entangled counterpart is investigated. The system presented here will find potential applications in long-distance quantum information processing.

PACS: 03.67.Bg, 03.67.Hk DOI: 10.1088/0256-307X/30/6/060302

For future long-distance quantum information processing networks,[1] quantum states need to be transferred with minimum disturbance between two or more parties who are far away from each other. Furthermore, faithful storing and retrieval of quantum states on demand is also required. Alkaline atoms that absorb and emit at wavelengths around 0.8 μm are strong candidates for quantum memory devices and have been employed to store optical quantum states. Current installed telecom optical fibers with the lowest loss band around 1.5 μm are suitable for the distribution of optical quantum states over long distances. In this case, one can benefit from the low linear loss of the fiber which is very desirable because any losses will inevitably introduce vacuum noise and deteriorate the quantum properties of vulnerable quantum states.

During the past few years, great progress has been seen on the generation of squeezed light at atomic wavelengths and telecom wavelengths, respectively. Squeezed light resonating with the rubidium (Rb) D1 line[2–7] or the cesium D2 line[8–11] has been obtained. Based on the atomic ensemble consisting of alkaline atoms, the quantum memories of squeezed vacuum and even a two-mode squeezed state were successfully demonstrated.[12–14] Squeezed light was also generated at the telecom band around 1.5 μm.[15–19] On the other hand, the two-color quantum entangled state at 0.8 and 1.5 μm has attracted particular interest recentlyl;[20–29] such entangled states can be utilized to make a connection between an alkaline-atom quantum memory device and a quantum communication device based on telecom optical fibers. In this Letter, we present a two-color continuous variable (CV) entangled source at the Rb D1 line (795 nm) and the telecom wavelength (1560 nm). The entanglement distribution is achieved by injecting the 1560 nm beam into a 5-km single mode fiber and the entanglement property between the distributed beam and the local beam is investigated. Furthermore, the frequency tunability of the entangled state is demonstrated by measuring the hyperfine transitions of the Rb D1 line based on saturated absorption spectroscopy.

The experimental setup is sketched in Fig. 1. A 526.5-nm single frequency laser was employed to pump a ring nonlinear resonator from two opposite directions. The ring entangler is in a bow tie configuration consisting of two spherical mirrors and two plane mirrors. A 20-mm-long periodically poled KTiOPO4 (PPKTP) was used as the nonlinear medium. In the forward direction, the nonlinear resonator operated as an above-threshold optical parametric oscillator (OPO) at a pump level approximately 1.2 times the oscillation threshold. The generated twin beams have three purposes: acting as local oscillator (LO) for homodyne detection, providing the 1560 nm seed field for the backward optical parametric amplifier (OPA), which is pumped below (0.6 times) the threshold, and supplying the 795 nm beam for wavelength tuning based on saturated absorption spectroscopy.

By utilizing the phase-insensitive signal-injected OPA, two-color CV entangled fields can be prepared robustly, i.e., the scheme eliminates the necessity of precise phase control between the signal and pump fields. Amplitude quadrature difference

*Supported by the National Natural Science Foundation of China under Grant No 11074156, the TYAL, the National Basic Research Program of China under Grant No 2010CB923101, the NSFC Project for Excellent Research Team under Grant No 61121064, and the Shanxi Scholarship Council of China.

**Corresponding author. Email: yongmin@sxu.edu.cn

(phase quadrature sum) noise power spectrum between down-converted fields at 795 and 1560 nm is recorded by using homodyne detection and a spectrum analyzer. The frequency tuning of the 795 nm beam to the hyperfine transitions of the Rb D1 line is performed as follows. Firstly, the oscillating wavelength of the 795 nm signal light was tuned coarsely within ±0.01 nm from the target wavelength by varying the temperature of the PPKTP crystal (the temperature tuning coefficient is about 0.2 nm per degree centigrade). Next, the signal wavelength was mode-hop tuned with a step size of one OPO free spectrum range (FSR, 950 MHz) by scanning the OPO cavity length at the fixed temperature (the overall mode-hop tuning range is approximately 0.2 nm when the cavity length varies half of the pump wavelength). During the above two steps the signal wavelength was monitored using a high-resolution wavelength meter. Once the signal wavelength falls within one FSR from the target wavelength, the OPO cavity length was actively locked to the selected signal-idler mode pair. Then, the saturated absorption spectrum was recorded by smooth scanning the signal frequency which was achieved by continuously tuning the pump laser. It is stressed here that the continuous tuning range of the 795 nm light field should be larger than the step size of the mode-hop tuning to ensure full wavelength coverage.

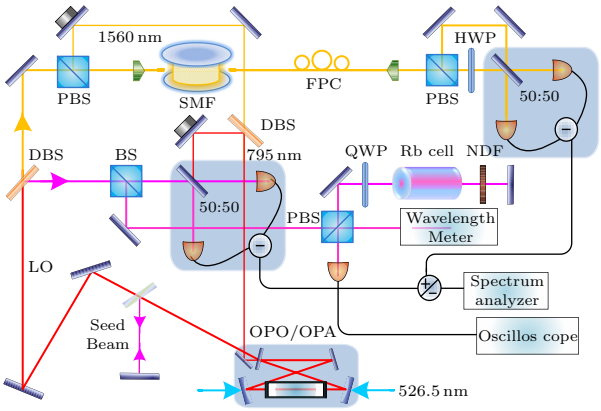

Fig. 1. (Color online) Schematic of the experimental setup. PBS: polarizing beam splitter; DBS: dichroic beam splitter; BS: beam splitter; LO: local oscillator; SMF: single-mode fiber; FPC: fiber polarization controller; HWP: half waveplate; QWP: quarter waveplate; NDF: neutral density filter.

For observation of the hyperfine level transition of Rb, a portion of the 795 nm beam was directed to a polarizing beam splitter (PBS) where part of the beam was injected into the wavelength meter and the rest was deflected to a Rb cell as a pump beam. After a double-pass through a neutral density filter, the pump beam was reflected back into the cell to act as a weak probe beam. The position of the quarter wave plate was chosen such that the probe beam goes straight through the PBS and was detected by a photodetector. Figure 2 shows the measured saturated absorption spectrum of hyperfine level transition for the Rb D1 line ($5S_{1/2}$–$5P_{1/2}$ transition). This transition is of great interest for its capability in the field of quantum memory.

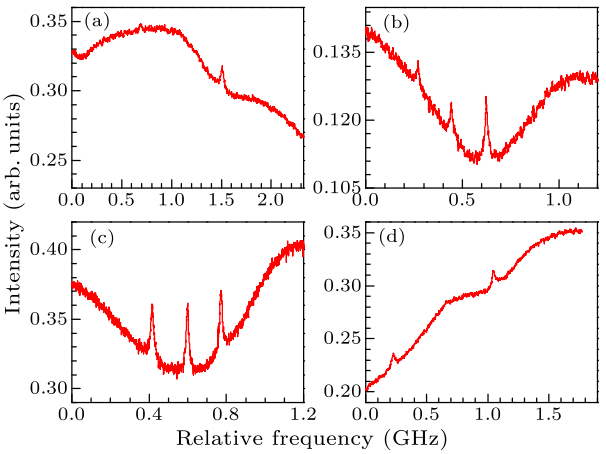

Fig. 2. (Color online) Saturated absorption spectra of hyperfine level transition for the Rb D1 line: (a) ^{87}Rb $5S_{1/2}(F = 1)$–$5P_{1/2}(F' = 1,1$ cross over $2,2)$, (b) ^{85}Rb $5S_{1/2}(F = 2)$–$5P_{1/2}(F' = 2,2$ cross over $3,3)$, (c) ^{85}Rb $5S_{1/2}(F = 3)$–$5P_{1/2}(F' = 2,2$ cross over $3,3)$, (d) ^{87}Rb $5S_{1/2}(F = 2)$–$5P_{1/2}(F' = 1,1$ cross over $2,2)$.

To realize quantum information processing tasks such as quantum teleportation and quantum cryptography, the distribution of entangled states over long distances is required.[30] Because the wavelength of one beam of the two-color entangled light lies in the telecom band, it is straightforward to utilize a standard single mode telecom fiber to transport the beam and distribute the entanglement. The single-mode fiber utilized here has a mode field diameter of 10.4 μm and numerical aperture of 0.12. The 1560 nm signal beam from the OPA was firstly collimated by a lens with focus length of 150 mm, and then an aspheric lens with focus length of 3.9 mm was used to precisely couple the beam into the fiber. At the output port of the fiber, an aspheric lens with focus length of 6.2 mm was used to collimate the beam emitting from the fiber. The single-path transmission efficiency for the fiber is determined by measuring the power in front of and behind the fiber. To avoid undesired polarization and phase drifts between the signal and LO over long-distance transmission, the LO and signal beams were combined on a PBS and were coupled into the same single mode fiber (polarization multiplexing). Due to the random fluctuations of birefringence of the ordinary single mode fiber, the polarization state will evolve rapidly as the light propagates along the fiber and the output polarization state will differ greatly from the linearly polarized input.[31] To compensate for such polarization state variation, an in-line fiber optic polarization controller was used to

restore linearly polarized light at the fiber output.

After leaving the fiber, the LO and the signal beam were polarization-demultiplexed by a PBS with an extinction ratio over 30 dB. Then the beams were directed to two input ports of a 50/50 beamsplitter for homodyne detection. In the first experiment, a short 1-m fiber was used and the single-path transmission efficiency was measured to be $85 \pm 1\%$. Figures 3(a) and 3(b) show the measured quantum correlations, the observed quantum correlations for the amplitude quadrature difference and phase quadrature sum are 1.9 dB and 1.8 dB, respectively, at analysis frequency around 3 MHz. In Fig. 3, electronic dark noise of 9 dB below the quantum noise limit (QNL) is not subtracted. The inseparability criteria are clearly violated by using the experimental values: $\langle[\Delta(\hat{X}_{795} - \hat{X}_{1560})]^2\rangle + \langle[\Delta(\hat{Y}_{795} + \hat{Y}_{1560})]^2\rangle = 1.31 < 2$,[32] where $\hat{X}_j$, $\hat{Y}_j$ (j = 795,1560) is amplitude and phase quadrature, respectively.

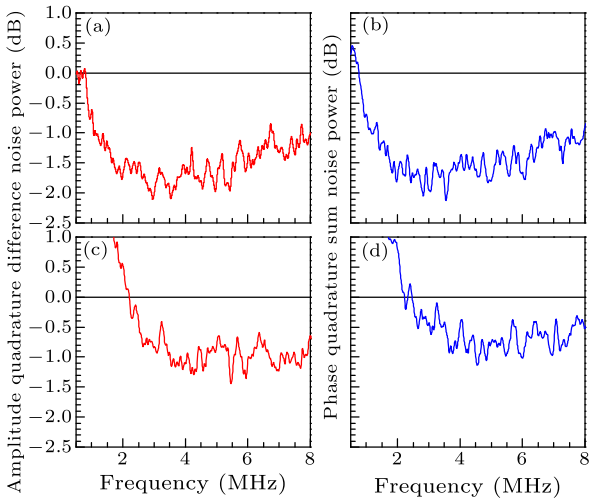

Fig. 3. (Color online) The normalized quadrature correlation noise spectrum of the entangled fields after the 1560 nm signal field transmitted through the single mode fibers. Here (a) and (b) show the noise spectrum for the 1-m single mode fiber; (c) and (d) illustrate the noise spectrum for the 5 km single mode fiber.

In the second experiment, a 5-km-long fiber was used to transport the 1560 nm signal field and demonstrates the entanglement distribution. The single-path transmission efficiency decreases to $65 \pm 1\%$ due to the loss of single mode fiber. In this case, the detected 795 nm photocurrent signal is delayed with 25.36 μs to synchronize the arrival times of the entangled beams to their photodetectors. The quantum correlation results are shown in Figs. 3(c) and 3(d), the observed quantum correlations for the amplitude quadrature difference and phase quadrature sum are 1.1 dB and 0.9 dB, respectively, at an analysis frequency of 5 MHz. The corresponding value of inseparability criteria becomes $\langle[\Delta(\hat{X}_{795} - \hat{X}'_{1560})]^2\rangle + \langle[\Delta(\hat{Y}_{795} + \hat{Y}'_{1560})]^2\rangle = 1.59 < 2$. The degradation of the quantum correlations are caused mainly by the linear loss introduced by the fiber and partly due to the phenomenon of guided acoustic wave Brillouin scattering (GAWBS) in the single mode fiber.[33]

Considering only the linear loss of the fiber, the measured quantum correlations can be modeled by a beam splitter with reflectivity of $1 - \eta$ ($\eta = \eta_2/\eta_1$). The amplitude and phase quadratures of the 1560 nm signal field at the 5 km fiber output can be given by

$$\begin{aligned} \hat{X}'_{1560} &= \sqrt{\eta}\hat{X}_{1560} + \sqrt{1-\eta}\hat{X}_{\rm V}, \\ \hat{Y}'_{1560} &= \sqrt{\eta}\hat{Y}_{1560} + \sqrt{1-\eta}\hat{Y}_{\rm V}, \end{aligned} \tag{1}$$

where $\hat{X}_{\rm V}$ and $\hat{Y}_{\rm V}$ are the amplitude and phase quadratures of the vacuum field. By using Eq. (1) and the experimental values (the analysis frequency is 5 MHz and the QNL has been normalized to 1 for the combination of quadratures): $\eta_1 = 0.85$, $\eta_2 = 0.65$, $\langle(\Delta\hat{X}_{795})^2\rangle = \langle(\Delta\hat{Y}_{795})^2\rangle = 1.00$, $\langle(\Delta\hat{X}_{1560})^2\rangle = \langle(\Delta\hat{Y}_{1560})^2\rangle = 0.86$, $\langle\Delta\hat{X}_{795}\Delta\hat{X}_{1560}\rangle = 0.592$, and $\langle\Delta\hat{Y}_{795}\Delta\hat{Y}_{1560}\rangle = -0.584$, the theoretical value of the inseparability criteria can be calculated by

$$\begin{aligned} &\langle[\Delta(\hat{X}_{795} - \hat{X}'_{1560})]^2\rangle + \langle[\Delta(\hat{Y}_{795} + \hat{Y}'_{1560})]^2\rangle \\ &= \langle(\Delta\hat{X}_{795})^2\rangle + \langle(\Delta\hat{X}'_{1560})^2\rangle - 2\langle\Delta\hat{X}_{795}\Delta\hat{X}'_{1560}\rangle \\ &\quad + \langle(\Delta\hat{Y}_{795})^2\rangle + \langle(\Delta\hat{Y}'_{1560})^2\rangle + 2\langle\Delta\hat{Y}_{795}\Delta\hat{Y}'_{1560}\rangle \\ &= 1.73. \end{aligned} \tag{2}$$

The theoretical result is in rough agreement with the observed value of 1.59.

Further experiments will be carried out to optimize the relevant parameters to obtain higher quantum correlation results. For instance, the fiber end faces can be antireflection coated to minimize the coupling loss for the 1560 nm light, and it is noted that single-path transmission efficiency of 95% has been obtained with this method.[34] Furthermore, homodyne detectors with ultra-low electrical noise will be designed and built, in this case, the power of 1560 nm LO can be decreased and the unwanted GAWBS noises will be suppressed.

The presented entangled source is compatible with electromagnetically induced transparency (EIT) based quantum memory in Rb atoms,[12,13,35] such quantum memory is narrowband with a bandwidth around 5.5 MHz.[28] The measured entanglement in the current system appears to be at a sideband frequency above 1 or 2 MHz. Although the degree of entanglement is expected theoretically to be higher in a low frequency range, there are several reasons[4,6,11] which result in the degradation of entanglement in practice, i.e., the large technical noise of a laser at low frequencies, the accuracy of the cavity and phase locking, and the common mode rejection ratio of homodyne detection at low frequencies. All these issues will introduce excess noises into the system and contaminate the entanglement in low frequency range. By

improving the accuracy of the locking system and the balance of homodyne detection, optimizing the seed power level, entanglement is readily accessible at frequencies below 1 MHz in current OPA system. Besides EIT based quantum memory, the presented entangled source is also compatible with the gradient echo memory scheme.[36,37] This type of scheme has a large bandwidth in principle which can be adjusted by the applied magnetic or electric broadening. To implement a quantum memory, the entangled source needs to be pulsed, which can be achieved by using an electro- or acousto-optical modulator or an ultrafast mechanical chopper.

In conclusion, a frequency-tunable two-color CV entangled state at Rb D1 line (795 nm) and telecom wavelength (1560 nm) has been demonstrated. The ability of continuous tuning enables the observation of the hyperfine transitions of Rb D1 lines based on saturated absorption spectroscopy. The long-distance distribution of the entangled state is achieved by utilizing a 5-km-long telecom single mode fiber. The system presented here will find potential applications in the realization of long-distance quantum information processing such as quantum cryptography and quantum teleportation, etc.

References

[1] Kimble H J 2008 *Nature* **453** 1023
[2] Akamatsu D et al 2004 *Phys. Rev. Lett.* **92** 203602
[3] Tanimura T et al 2006 *Opt. Lett.* **31** 2344
[4] Hetet G et al 2007 *J. Phys. B: At. Mol. Opt. Phys.* **40** 221
[5] McCormick C F et al 2007 *Opt. Lett.* **32** 178
[6] Predojević A et al 2008 *Phys. Rev.* A **78** 063820
[7] Mikhailov E E et al 2008 *Opt. Lett.* **33** 1213
[8] Polzik E S 1992 *Phys. Rev. Lett.* **68** 3020
[9] Marin F et al 1997 *Opt. Commun.* **140** 146
[10] Neergaard-Nielsen J S et al 2006 *Phys. Rev. Lett.* **97** 083604
[11] Burks S et al 2009 *Opt. Express* **17** 3777
[12] Honda K et al 2008 *Phys. Rev. Lett.* **100** 093601
[13] Appel J et al 2008 *Phys. Rev. Lett.* **100** 093602
[14] Jensen K et al 2011 *Nat. Phys.* **7** 13
[15] Silberhorn C et al 2001 *Phys. Rev. Lett.* **86** 4267
[16] Nishizawa N et al 2002 *Jpn. J. Appl. Phys. Part 2* **41** L130
[17] Eto Y et al 2007 *Opt. Lett.* **32** 1698
[18] Feng J X et al 2008 *Appl. Phys. Lett.* **92** 221102
[19] Mehmet M et al 2011 *Opt. Express* **19** 25763
[20] Schori C et al 2002 *Phys. Rev.* A **66** 033802
[21] Villar A S et al 2005 *Phys. Rev. Lett.* **95** 243603
[22] Su X L et al 2006 *Opt. Lett.* **31** 1133
[23] Jing J et al 2006 *Phys. Rev.* A **74** 041804(R)
[24] Grosse N B et al 2008 *Phys. Rev. Lett.* **100** 243601
[25] Coelho A S et al 2009 *Science* **326** 823
[26] Li Y M et al 2010 *Appl. Phys. Lett.* **97** 031107
[27] Samblowski A et al 2010 arXiv:1011.5766v2 [quant-ph]
[28] Guo X M et al 2011 *Phys. Rev.* A **84** 020301(R)
[29] Guo X M et al 2012 *Appl. Phys. Lett.* **100** 091112
[30] Madsen L S et al 2012 *Nat. Commun.* **3** 1083
[31] VanWiggeren G D et al 1999 *Appl. Opt.* **38** 3888
[32] Duan L M et al 2000 *Phys. Rev. Lett.* **84** 2722
[33] Shelby R M et al 1985 *Phys. Rev. Lett.* **54** 939
[34] Mehmet M et al 2010 *Opt. Lett.* **35** 1665
[35] Zhang H et al 2011 *Nat. Photon.* **5** 628
[36] Hosseini M et al 2011 *Nat. Phys.* **7** 794
[37] Hedges M P et al 2010 *Nature* **465** 1052